Polish Society of Composite Materials
Polskie Towarzystwo Materiałów Kompozytowych
19: 4 (2019) 169-173
COMPOSITES THEORY AND PRACTICE
ISSN: 2084-6096
ISSN (online): 2299-128X

**Olena Poliarus[1*], Oleksandr Umanskyi[1], Jerzy Morgiel[2], Piotr Bobrowski[2], Maciek Szlezyner[2]
Tetiana Mosina[1], Iryna Martsenyuk[1]**

[1]Frantsevich Institute for Problems of Materials Science, National Academy of Sciences of Ukraine (IPMS NASU), Krzhyzhanovsky St. 3, 03142 Kyiv, Ukraine
[2]Institute of Metallurgy and Materials Science, Polish Academy of Sciences (IMIM PAN), ul. Reymonta 25, 30-059 Krakow, Poland
** Corresponding author: E-mail: elena_polyarus@ukr.net*

Received (Otrzymano) 17.12.2019

STRUCTURE AND STRENGTH CHARACTERISTICS OF NiAl-BASED COMPOSITE MATERIALS

In this paper, the structure of NiAl-15wt.%CrB_2, NiAl-15wt.%ZrB_2 and NiAl-15wt.%TiB_2 composite compact materials was studied using SEM. The composites were obtained by sintering in vacuum. The phase composition was studied by XRD analysis. The effect of the diboride additives on the NiAl hardness was studied. It is shown that the initial intermetallic had a hardness of 288 HV20. At the same time, the hardness value for the NiAl-15wt.% ZrB_2 composite is 349 HV20, for NiAl-15wt.%TiB_2 it is 392 HV20 and for the NiAl-15wt.%CrB_2 composite material it is 468 HV20.

Keywords: NiAl intermetallic, CrB_2, sintering, structure, hardness, microfragility, microstrength

INTRODUCTION

The direction of the development of new composite materials intended for use in demanding operating conditions, is one of the most perspective in modern materials science. The main focus is on the development of composites based on metals or alloys dispersed with refractory compounds (oxides, carbides, nitrides or borides) [1-4]. In order to obtain high performance characteristics of composites designed to work under conditions of slip friction, it is rational to use materials with high corrosion resistance, in particular nickel aluminide [5]. However, its use as a high-temperature structural material in friction units is limited due to its intense plastic deformation at temperatures above 500°C. One of the ways to increase the high-temperature strength of nickel aluminide is its hardening by refractory compounds, in particular borides. It has been found that an optimum refractory additive for the production of NiAl-based composites is chromium diboride [6].

The aim of this work was to investigate the structure and mechanical characteristics of NiAl-CrB_2, NiAl-15wt.%ZrB_2 and NiAl-15wt.%TiB_2 composite materials.

EXPERIMENTAL TECHNIQUES

Commercial powders of the NiAl intermetallic compound and diborides (CrB_2, TiB_2, ZrB_2) supplied respectively by Polema JSC were used as the base materials. The powder particle sizes of the initial components were 40 micrometers for the intermetallic compound and 20 micrometers for the diborides.

The composite materials based on the NiAl-MeB_2 system were obtained by vacuum sintering at T = = 1650°C of a mixture of the initial components. The porosity value for all the composites was ~ 5%.

Composites phase analyses were conducted by means of X-ray phase analysis. Filtered CoKα radiation was used. Remote control of the measurement, and data processing are realized by means of a computer system, which uses APD (Philips) or DIFFRACplus (Bruker AXS) programs and the ICDD crystallographic database.

Hardness tests were conducted using a FALCON 509 Vickers hardness tester (Innovatest). The HV parameter was measured under a 20 kg force.

Microfragility (γ) and microstrength (σ) were calculated using formulas:

$$\gamma = \frac{D^2 - d^2}{d^2} \text{ and } \sigma = \frac{1000 \cdot P}{D^2}$$

where: D^2 - the maximum diameter of the brittle damage zone around the indenter print [μm]; d^2 - the average size of the damage zone [μm]; P - Indenter load [N].

The microstructure, and chemical composition of the composite materials were researched using an FEI Quanta 3D FEG dual beam high-resolution scanning electron microscope integrated with the EDAX Trident system (an Apollo 40 EDS spectrometer, a TEXS WDXS spectrometer and a Hikari EBSD camera) and a PHILIPS XL30 scanning electron microscope equipped with a LINK ISIS energy dispersive X-ray spectrometer, Oxford Instruments.

RESULTS AND DISCUSSION

The microstructure of the compact composite samples (Fig. 1) is characterized by a mainly uniform distribution of diboride grains (2) in the intermetallic matrix (1).

a)
b)
c)
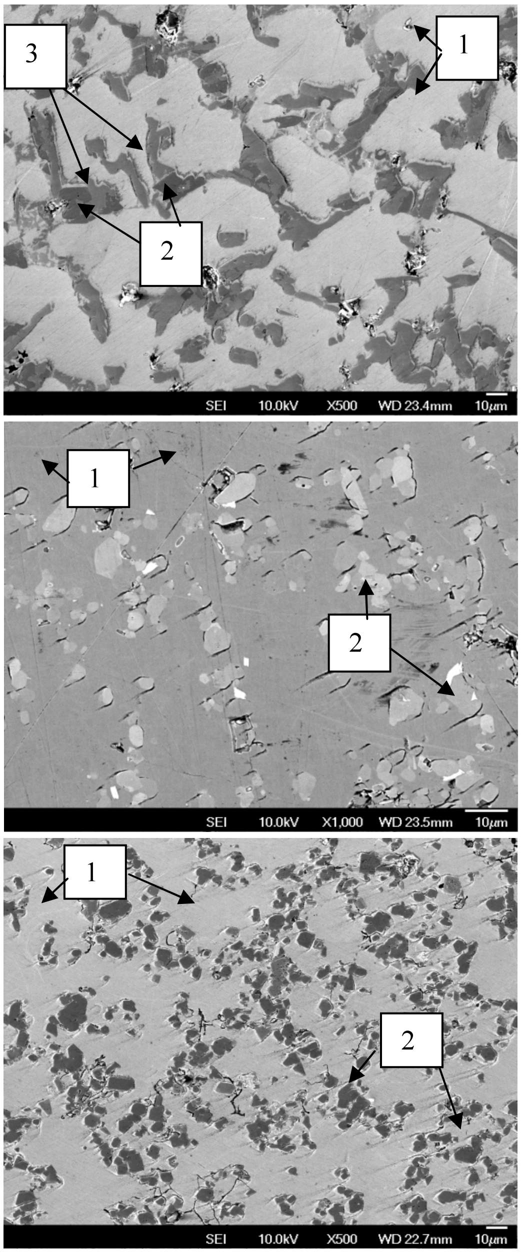

Fig. 1. SEM micrographs of compact composite materials: NiAl-15 wt.%CrB_2 (a); NiAl-15 wt.%ZrB_2 (b); NiAl-15wt.%TiB_2 (c); 1 - intermetallic matrix (NiAl); 2 - diboride grains (2a - CrB_2, 2b - ZrB_2, 2c - TiB_2), 3 - new boride phase

According to the microstructures of all the materials, the NiAl-15wt.%ZrB_2 (Fig. 1b) and NiAl-15wt.%TiB_2 composites (Fig. 1c) are characterized by the presence of cracks. This result can be explained by the difference in the thermal expansion coefficient of the starting materials (CTE for NiAl = $13 \cdot 10^{6}$°C^{-1}, for ZrB_2 = = $5.9 \cdot 10^{6}$°C^{-1}, for TiB_2 = $8.1 \cdot 10^{6}$°C^{-1}). In the process of heating and cooling the materials during sintering, this leads to the formation of cracks at the matrix - boride grain boundary.

For the NiAl-15 wt.%CrB_2 composite (Fig. 1a) a new boride phase (3) is formed because of the physical-chemical interaction between the initial components. This phase is intermediate between the intermetallic matrix and the refractory inclusions that can promote better bonding between the initial components. The microhardness of the new boride phase is ~ 9÷11 GPa. The presence of an additional strengthening phase in the material structure in the future should give a positive impact on the mechanical characteristics of the materials. Furthermore, the presence of an intermediate phase is also useful in terms of compensating for differences in the CTE of the metallic and refractory phases (CTE for CrB_2 = $10.5 \cdot 10^{6}$°C^{-1}).

According the SEM analysis results of the NiAl-15wt.%CrB_2 composite (Fig. 2) we can see two different boride grain shapes in its structure (Fig. 2a,b). The presence of some grains with a lineal form (Fig. 2b) in the composite structure is related to secondary boride phases forming during the sintering process.

a)
b)
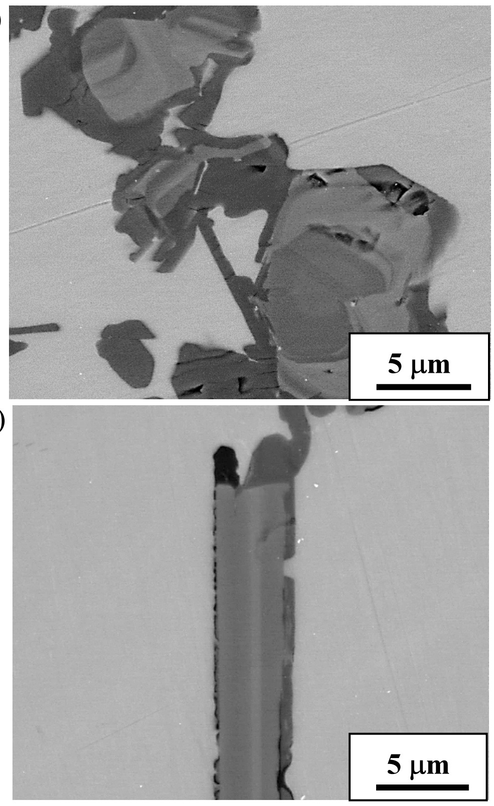

Fig. 2. SEM micrographs of sintered NiAl-15wt.%CrB_2 composite material

To investigate the phase formation of the NiAl-15wt.%CrB_2 composite materials, integrated XRD analyses were performed.

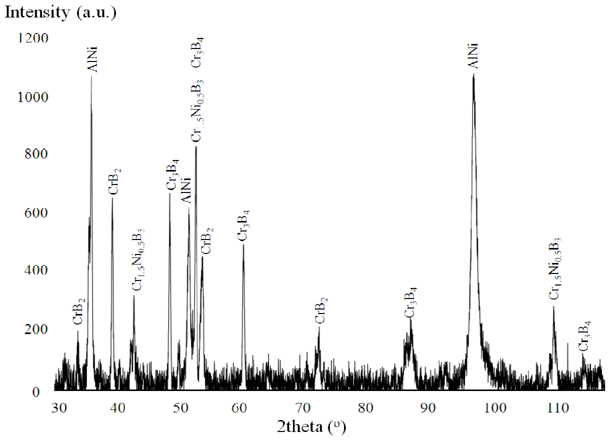

Fig. 3. XRD results of NiAl-15wt.%CrB_2 sintered composite material

According to the XRD results (Fig. 3), the developed composite material consists of three main phases: initial intermetallic (AlNi), chromium borides (CrB_2, Cr_3B_4) and $Cr_{1.5}Ni_{0.5}B_3$.

Since the materials are designed to work in highly stressed units, the strength characteristics (Figs. 4 and 5) were investigated (like hardness, microfragility and microstrength).

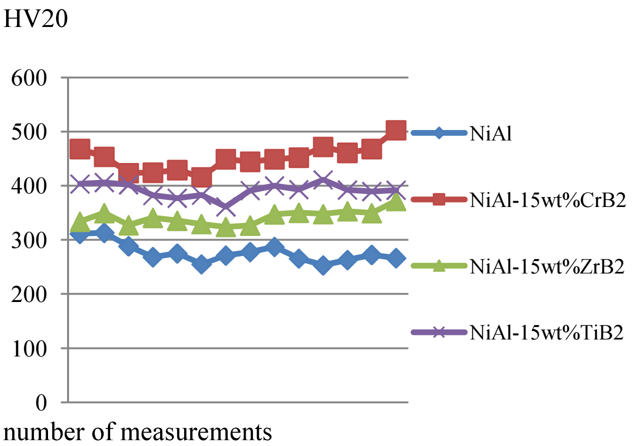

Fig. 4. Hardness diagram of initial NiAl and developed composite materials

According to the experiment data, the lowest hardness value was exhibited by the initial intermetallic compound and is 288 HV20. The obtained hardness results of the intermetallic correlate with the literature data [8-10]. For the developed composite materials, the hardness values are 349 HV20 for NiAl-15wt.%ZrB_2, 392 and 468 HV20 for NiAl-15wt.%TiB_2 and NiAl-15wt.%CrB_2 respectively. Thus, the hardness tests results showed that the HV/20 parameter of the developed composite is 1.2-1.6 times higher than that of the intermetallic compound (Fig. 4).

The obtained results are confirmed by the corresponding microstructures of the materials after testing, crack distribution on the initial NiAl and the developed composites (Fig. 5), as well as by calculations of the microfragility (γ) and microstrength (σ).

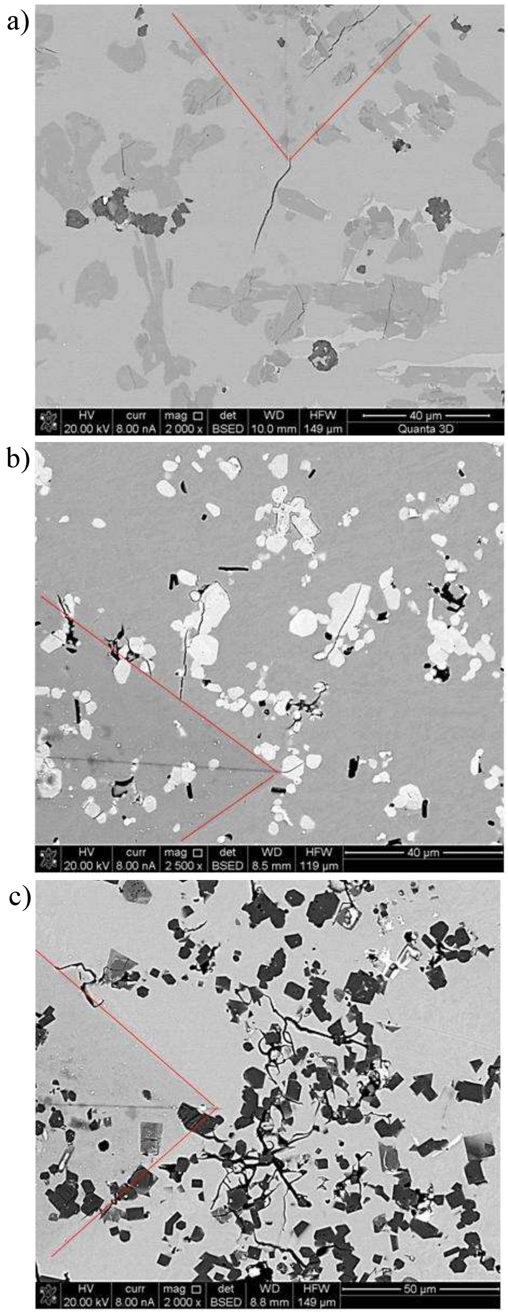

Fig. 5. Crack distribution on initial NiAl and developed composite materials after hardness test: a) NiAl-15wt.%CrB_2, b) NiAl-15wt.%ZrB_2, c) NiAl-15wt.%TiB_2

The crack propagation for the NiAl-15wt.%CrB_2 composite (Fig. 5a) has a classic appearance - the crack begins at the top of the imprint and spreads through the intermetallic matrix. The formation of cracks on the boride grains near the imprint is also observed. At the same time, the values of microfragility and microstrength for this material are $\gamma = 0.51$ and $\sigma = 1.63$ N/µm^2, respectively.

The NiAl-15wt.%ZrB_2 composite (Fig. 5b) is characterized by the formation of cracks, both at the top of the imprint and along its faces. However, the formation of cracks on the boride grains is also observed. The microfragility of such a composite is 1.29, and the microstrength is 0.94 N/µm^2.

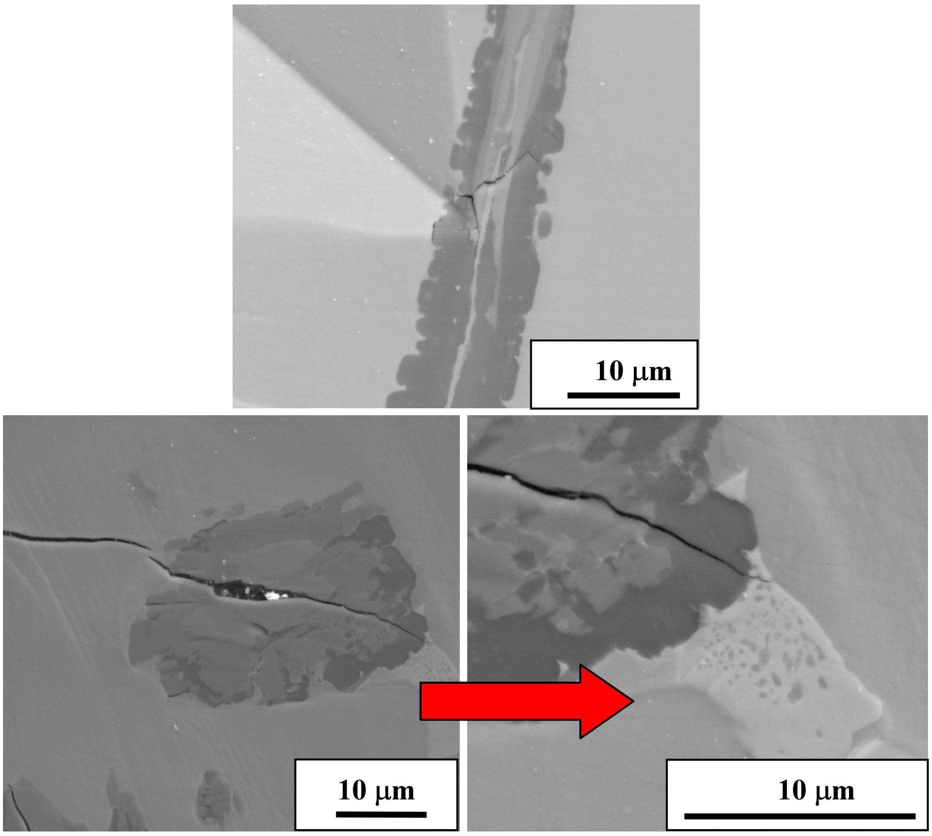

Fig. 6. SEM micrographs of crack distribution in sintered NiAl-15 wt.%CrB_2 composite material after hardness tests

For the NiAl-15 wt.% TiB_2 composite (Fig. 5c), crack propagation is completely different. The cracks in this material begin on the titanium diboride grains and spread to the nearest boride grains, covering a large area. The values of micro-fragility and micro-strength for this composite are equal to γ = 0.95 and σ = 0.92 N/μm^2, respectively.

More detailed investigations of the nature of the crack distribution of the NiAl-15wt.%CrB_2 composite (Fig. 6) showed that the chromium boride grains in the structure of this material act hinder the further spread of cracks. Thus, the chromium diboride in the nickel aluminide counteracts the spread of cracks, which leads to a significant increase in the strength of the material.

SUMMARY

The structure of NiAl-15wt.%CrB_2, NiAl-15wt.%ZrB_2 and NiAl-15wt.%TiB_2 composite materials was studied. It is shown that the formation of additional Cr_3B_4 and $Cr_{1.5}Ni_{0.5}B_3$ boride phases occurs during the preparation of NiAl-15wt.%CrB_2 composites.

The effect of the diboride additives on the hardness of the intermetallic compound was studied. It was found that the NiAl-15wt.%CrB_2 composite material hardness is 1.6 times higher than the hardness of the initial intermetallic compound. Investigations of the nature of the crack distribution showed that the chromium diboride grains in the structure of the composite material impede the further spread of cracks.

Acknowledgments

This work was supported by the agreement on scientific cooperation between the Institute of Metallurgy and Materials Science, Polish Academy of Sciences and Frantsevich Institute for Problems of Materials Science, National Academy of Sciences of the Ukraine

REFERENCES

[1] Whittenberger J.D., Viswanadham R.K., Mannan S.K., Sprissler B., Elevated temperature slow plastic deformation of NiAl-TiB_2 particulate composites at 1200 and 1300 K, J. Mater. Sci. 1990, 25, 35-44.

[2] Whittenberger J.D., Kumar S., Mannan S.K., Viswanadham R.K., Slow plastic deformation of extruded NiAl-10TiB_2 particulate composites at 1200 and 1300 K, J. Mater. Sci. Lett. 1990, 9, 326-328.

[3] Sheng L.Y., Yang F., Xi T.F., Guo J.T., Investigation on microstructure and wear behavior of the NiAl-TiC-Al_2O_3 composite fabricated by self-propagation high-temperature synthesis with extrusion, J. Alloys Compd. 2013, 554, 182-188.

[4] Umanskyi O., Poliarus O., Ukrainets M., Martsenyuk I., Effect of ZrB_2, CrB_2 and TiB_2 Additives on the tribological characteristics of NiAl-based gas-thermal coatings, Key Eng. Mater. 2014, 604, 20-23.

[5] Miracle D.B., Darolia R., NiAl and its Alloys, Structural applications of intermetallic compounds, ed. J.H. Westbrook, R.L. Fleischer, John Wiley & Sons, New York 2000, 20.

[6] Umanskyi O., Poliarus O.M., Ukrainets M.A., Physical-chemical interaction in NiAl-MeB_2 systems intended for

tribological applications, Welding Journal 2015, 94, 225--230.

[7] Chang S.T. et al., Effect of surface grinding on the strength of NiAl and Al_2O_3/NiAl composites, Mater. Chem. Phys. 1999, 59, 3. 220-224.

[8] Cymerman K., Michalski A., Spieki NiAl i Ni_3Al wytwarzane w reakcji SHS metodą PPS, Materialy Ceramiczne 2014, 66, 1, 4-9.

[9] Zhu S., Tribological behavior of NiAl matrix composites with addition of oxides at high temperatures, Wear 2012, 274-275, 423-434.

[10] Zhang Z.Y., Effects of Dy on the microstructure and hardness of NiAl alloys, Mater. Sci. Forum. 2013, 747-748, 788-796.

